Int. J. Heat Mass Transfer. Vol. 35, No. 1, pp. 73–86, 1992
Printed in Great Britain

0017-9310/92 $5.00 + 0.00

Wall temperature patterns in nucleate boiling

D. B. R. KENNING
Department of Engineering Science, Oxford University, Parks Road, Oxford OX1 3PJ, U.K.

(*Received February* 1991 *and in final form* 1 *March* 1991)

Abstract—Temperature patterns on the back of a thin stainless steel heated plate during pool nucleate boiling of water have been measured with thermochromic liquid crystal. It is shown that spatial variations which are large fractions of the mean wall superheat are to be expected in many experimental and industrial applications of boiling. They can cause errors in the measurement of the mean wall superheat by some conventional methods. Established mechanistic models which assume uniformity of wall superheat cannot represent correctly the processes controlling the density and intermittent activity of bubble nucleation sites on walls of finite thermal conductivity. The essential features of a realistic model are described.

1. INTRODUCTION

DESPITE decades of research there is as yet no comprehensive theoretical model for nucleate boiling heat transfer. Dhir [1] ended his recent exhaustive review with a call for a return to basic experiments with new techniques. This disappointing state of affairs may be a measure of the complexity of the boiling process. It may also indicate that some fundamental characteristic of the process has been neglected. In this paper it is argued that insufficient attention has been paid to the large spatial variations in wall superheat that may occur in the 'isolated bubble' regime.

Firstly, experimental evidence is presented to confirm that large spatial variations in wall superheat do occur. The experimental conditions are typical of the many simple pool boiling experiments from which the current understanding of nucleate boiling has been derived: water boiling at 100 kPa pressure on a thin stainless steel plate at a heat flux of 100 kW m^{-2}. The wall superheat has a spatially-averaged value of 20 K but the local values of superheat range from 4 to 30 K over distances of a few millimetres. The temperature distributions are determined from photographs of thermochromic liquid crystal spread on the rear surface of the heated plate, a technique pioneered by Raad and Myers [2] in 1971. Their liquid crystal had a colour play range of only 2 K and could not reveal spatial variations of the magnitude observed in the present study using material with colour play over the temperature span 104–132°C.

The liquid crystal technique can only be used on a thin boiling plate (in this case 0.13 mm thick), if the temperature distribution on the rear adiabatic surface is to be a good approximation to the temperature distribution at the boiling fluid/solid interface. The large spatial variations that are revealed might therefore be specific to experiments on thin, electrically-heated plates of low thermal conductivity. This possibility was investigated [3, 4] using a simple theoretical model for time-averaged conduction in a cylindrical region of wall round a nucleation site removing heat uniformly over an annular area of influence. It was shown that significant spatial variations in wall superheat may be expected on thick plates of materials such as stainless steel, their magnitude being sensitive to the size of the area of influence relative to the spacing between sites; much smaller variations occur on thick copper plates. The experimental observations show that the time-averaged steady-conduction model is oversimplified: the variations in wall superheat may cause time-dependent interactions with cycles of activity and quiescence at individual nucleation sites, as discussed in ref. [4]. The observations also illustrate the sensitivity of nucleate boiling to physico-chemical influences: different methods of cleaning the boiling surface, altering its wetting characteristics, caused radical changes in the nature of the space–time pattern of wall superheat going far beyond a simple change in the number of active sites.

Having confirmed that variations in wall superheat that are large fractions of the space–time average value can occur in nucleate boiling, the implications for experimental methods of measuring wall superheat and for theoretical models are discussed in the remainder of the paper. It is shown that some conventional experimental techniques can lead to substantial errors in the measurement of mean wall superheat in the presence of spatial variations. Long-established theoretical models with a mechanistic base, such as the Mikic and Rohsenow model [5], which consider only mean wall superheat without taking account of the spatial variations, do not correctly represent important physical processes which control the population of active nucleation sites on walls of finite thermal conductivity. The non-uniformities in wall superheat caused by any existing population of active sites must distort the probability of activation of new sites and influence the conditions for sites to remain active, sometimes causing sites to operate intermittently.

NOMENCLATURE

a	non-dimensional inner radius of area of influence
b	non-dimensional outer radius of area of influence
c	dimensional constant, equation (1)
d	non-dimensional wall thickness
k	thermal conductivity [$W m^{-1} K^{-1}$]
K	ratio of area of influence to bubble projected area
m	exponent, equation (1)
N	active nucleation site density [sites m^{-2}]
N'	potential nucleation site density [sites m^{-2}]
r	non-dimensional radial coordinate
r'	equivalent radius of nucleation site [m]
R	maximum bubble radius [m]
S	radius of conduction domain, $(\pi N)^{-1/2}$ [m]
t	local temperature [°C or K]
T	mean surface superheat [K]
T_a	activation superheat [K]
T_c	cessation superheat [K]
T_e	equilibrium superheat [K]
z	non-dimensional axial coordinate.

Greek symbols

α	thermal diffusivity [$m^2 s^{-1}$]
β	thermal coefficient of electrical resistivity [K^{-1}]
Δ	surface superheat range [K]
Θ	characteristic temperature difference, qS/k [K]
ϕ	heat flow per site whilst active [W]
ω	bubble frequency [rad s^{-1}].

2. EXPERIMENTS

2.1. *Experimental methods*

The boiling water was contained in a glass cell of rectangular cross-section 46 × 103 mm, 100 mm high, open to the atmosphere. The depth of the water was maintained at 40 mm. The heated surface was a horizontal stainless steel plate 0.13 mm thick, set into a layer of silicone rubber covering the base of the cell. Heavy brass electrodes soldered to the ends of the plate were supplied with ripple-free d.c. electrical power from a rotary generator. The heated area measured 39.3 × 28.2 mm.

The bottom of the cell was cut away over a strip 20 mm wide to expose the rear surface of the heated plate for the application of thermochromic liquid crystal, which indicates temperature by selective reflection of white light. The plate was coated with matt black enamel, then baked at 120°C for 72 h to remove all traces of solvent. A thin layer of liquid crystal was applied by brushing (with the plate held at 90°C to assist spreading), then covered with a layer of thin melinex film. The film protects the liquid crystal and promotes the formation of the colour-active Grandjean texture. Unencapsulated liquid crystal displays brighter colours than encapsulated material, but is more sensitive to the angles of illumination and viewing and to contamination. At present encapsulated material is not readily available for operating temperatures above 100°C, although no doubt this situation will change. Light from a narrow-beam (7°) tungsten–halogen lamp was directed onto the liquid crystal layer at an angle of 7° from the normal by a beamsplitter plate. The colour play was photographed through the beamsplitter with a 35 mm camera at a shutter speed of 1/500 s on ISO 200/24° colour print film. In order to calibrate colour against temperature, a similar layer of liquid crystal was applied to the base of a brass cylinder equipped with an electrical heater and a thermocouple, which was put in the place of the boiling plate in the same illumination. The colour was recorded at intervals of 2 K over the range 100–134°C.

The response of the liquid crystal on the rear surface of the boiling plate to the temperature signals generated at the front surface was governed in this case by thermal diffusion through the stainless steel plate, with an upper limit of about 20 Hz for negligible attenuation and phase shift. Ireland and Jones [6] have shown that an encapsulated liquid crystal layer 10 μm thick responds to a step change in substrate temperature within 3 ms. The response of an unencapsulated layer is similar, governed by thermal diffusion through the layer provided the crystal is within its colour play range [7]; for a crystal initially outside this range the latent heat of phase change would slow the response.

The stainless steel boiling plate, cut from hard-rolled sheet, was not subjected to any special preparation other than cleaning. The three tests reported here all followed the same procedure except for the method of cleaning. The cell was filled to a depth of 40 mm with cold demineralized water. The power was turned on at 150 kW m^{-2}. Small gas bubbles grew on the heater and were eventually dislodged as boiling developed. Vigorous saturated boiling was established after 10 min. Some very small gas bubbles remained suspended in the liquid circulating in the cell. After a further 3 min the heat flux was reduced to 100 kW m^{-2}, for which the bulk temperature was 98.3°C. Photographs of the liquid crystal were taken at intervals of 10 s providing random samples of the instantaneous temperature distributions on the rear surface of the boiling plate. The liquid crystal was also observed through the camera viewfinder. In the pre-

Figure 1. Test A

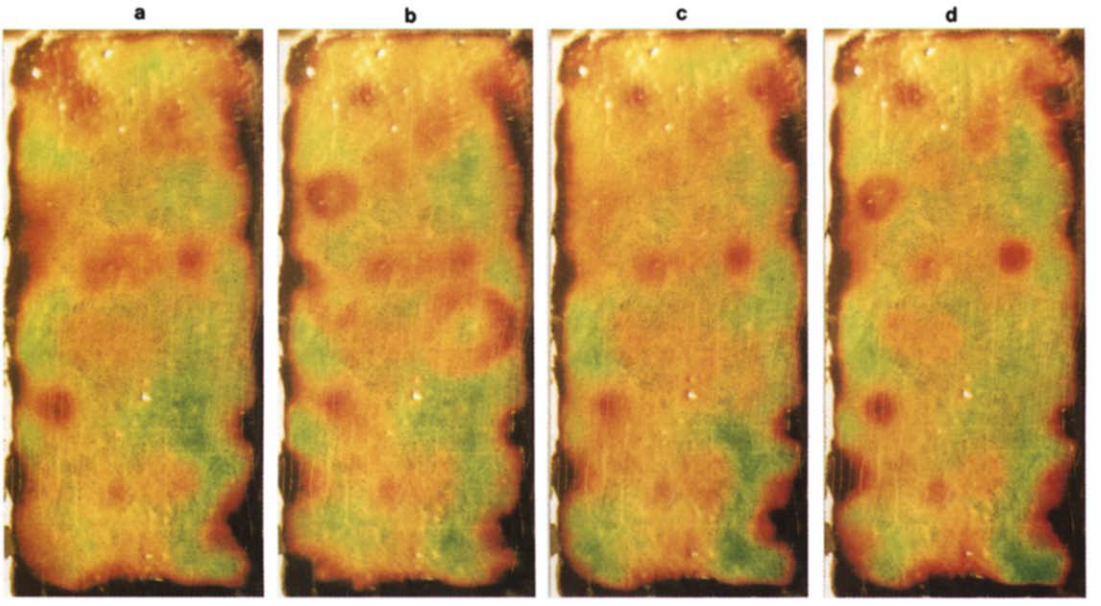

FIG. 1.

Figure 2. Test B

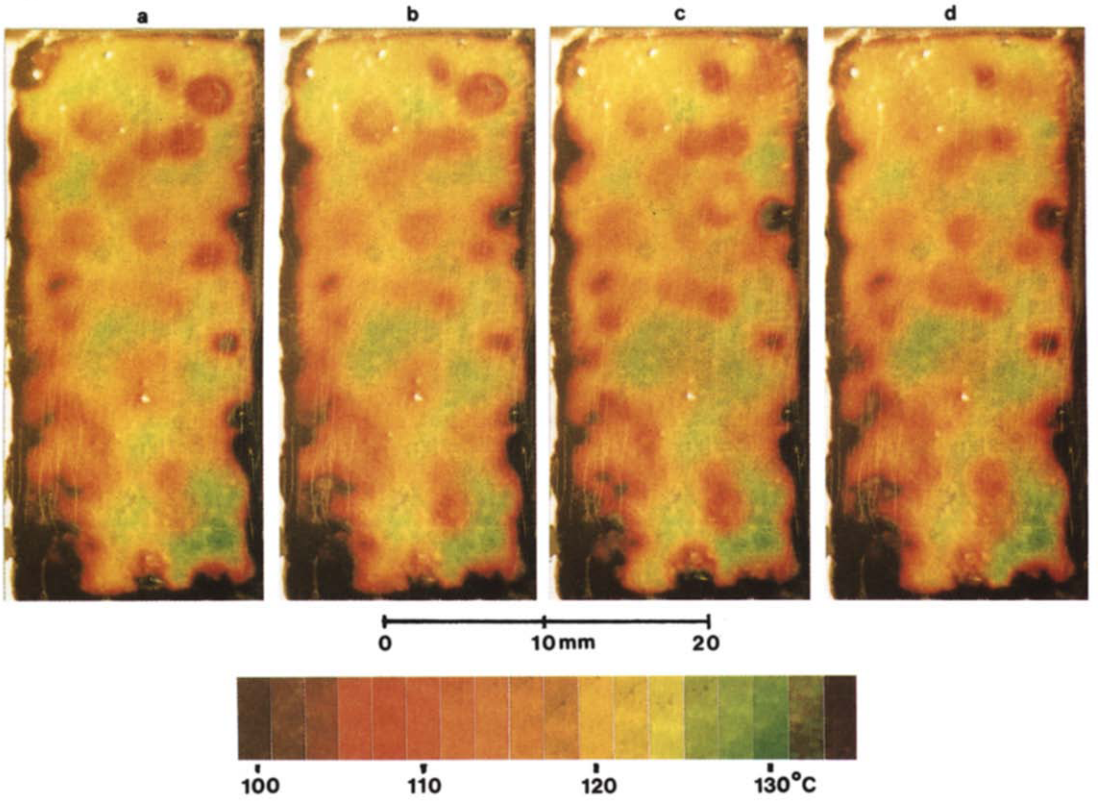

FIG. 2.

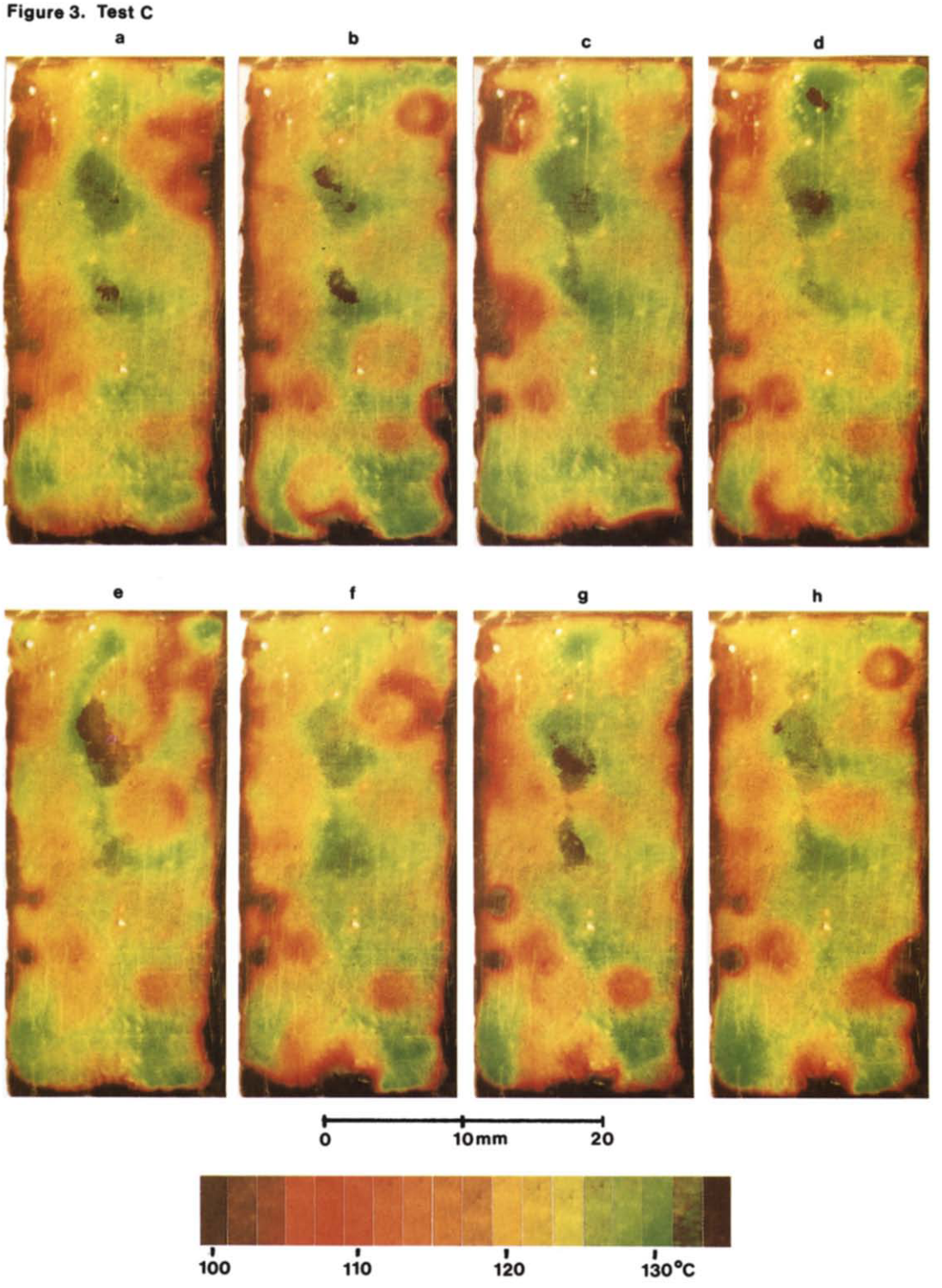

FIG. 3.

liminary tests described here no attempt was made to obtain continuous records of the temperature variations or of the bubble motion.

2.2. *Experimental observations*

Test A was performed after prolonged periods of boiling during the initial setting up of the system. The cell was emptied and immediately refilled without cleaning the boiling surface. Four representative photographs of the liquid crystal layer on the rear of the plate are shown in Fig. 1. Temperatures range from cold (red) spots at 108°C to hot (green) patches at 130°C. Common features are recognizable in the four photographs but there are also significant differences, such as the large cold ring 5.7 mm in diameter in Fig. 1(b). Visual observation gave the impression of a fairly steady pattern on which were superimposed momentary local splashes of red. Observing the boiling process itself revealed a mixture of stable sites producing continuous streams of bubbles 1–2 mm in diameter and other sites producing much larger (about 5 mm) single bubbles, or short bursts of a few bubbles, at irregular intervals.

Test B was performed after the boiling surface had been wiped with 'Genklene' (stabilized trichloroethane), followed by rinsing in hot water and finally demineralized water. This treatment left the surface in a poorly-wetted condition. Many small bubbles formed on the surface during the initial heating period preceding boiling. The temperature patterns in the four photographs in Fig. 2 are very similar. Visual observation gave the impression of a very steady pattern, with a slight flickering effect at some of the red spots. The nucleation sites on the boiling surface all appeared to be producing steady streams of small bubbles at high frequency.

Test C was performed after the boiling surface had been cleaned with 'Decon 90' residue-free detergent, followed by rinsing in hot water and demineralized water. This treatment left the surface in a highly-wetted condition so that it remained coated with a thin film of water prior to refilling the boiling cell. Very few gas bubbles appeared during the heating period preceding boiling. The temperature pattern during boiling fluctuated wildly so that the eight photographs in Fig. 3 appear at first sight to have few features in common. The cooler regions are mostly large red or orange rings with hotter centres; by examining 16 photographs it was established that the rings reappeared at preferred sites. There are black regions indicating heating of the liquid crystal beyond its colour play limit of 132°C. Visual observation confirmed the unsteady nature of the temperature pattern: short-lived flashes of red and orange and longer-lived patches of black appeared on a green background. Only a few nucleation sites could be seen on the boiling surface at any instant. They all produced large bubbles irregularly, one or two at a time followed by a period of quiescence.

2.3. *Analysis*

The objective of this preliminary work was to demonstrate the general nature and order of magnitude of the wall temperature variations so the conversion of liquid crystal colour to temperature was performed approximately by eye. The colour play range was divided into five bands: 101–107 (brown–red), 107–113 (red), 113–119 (orange), 119–125 (yellow), 125–131 (green). Dividing contours were traced from the photographs in an area of 4 cm^2 excluding the edges of the coated region. The areas corresponding to each band were measured, giving the histograms shown in Fig. 4. Because of the large variability in Test C the measurements from four photographs were averaged. The mean wall superheats and standard deviations were Test A 21 (5) K, Test B 20 (7) K, Test C 23 (5) K.

The centres of cold spots and rings were assumed to coincide with nucleation sites. In the area of 4 cm^2 19 sites were identified in Test A, 24 in Test B and 22 in Test C. (In Test C one photograph would typically show traces of only four or five sites so 16 photographs were examined. Each site appeared in at least two photographs.) Of the total of 45 sites only six were active in all three tests, eight were active in two out of three tests and 31 were active in one test only, Fig. 5.

3. DISCUSSION

3.1. *Nucleate boiling on thin plates*

The experiments have demonstrated that the local wall superheat can range from 20 to 150% of the spatial mean value. The temporal pattern of variation was strongly influenced by the wettability of the surface. When the surface was rendered poorly-wetted a large population of sites was continuously active: the temperature pattern was steady, with small superimposed fluctuations at the high frequency of bubble production. When the same surface was well-wetted few sites were active at any instant and individual sites emitted much larger bubbles intermittently. Consequently the temperature pattern was unsteady, with low frequency variations of large amplitude. Repeated sampling indicated that bubble activity was associated with particular sites so it is unlikely that it was caused by the random deposition on the surface of entrained gas or vapour microbubbles as suggested by Myers [8]. Although far fewer sites were active at any instant when the surface was well-wetted in Test C than when it was poorly-wetted in Test B, the total number of sites participating over a long period was similar. This is surprising, given the large effect of changes in contact angle on the population of gas bubble nucleation sites in supersaturated solutions of nitrogen in ethanol–water mixtures [9]. The sites active in Test C might be expected to be a small sub-set of the sites active in Tests A and B. In fact 10 of the 22 sites active at some time during Test C were new sites, which had not been activated in the preceding tests under what should have been more favourable conditions. This

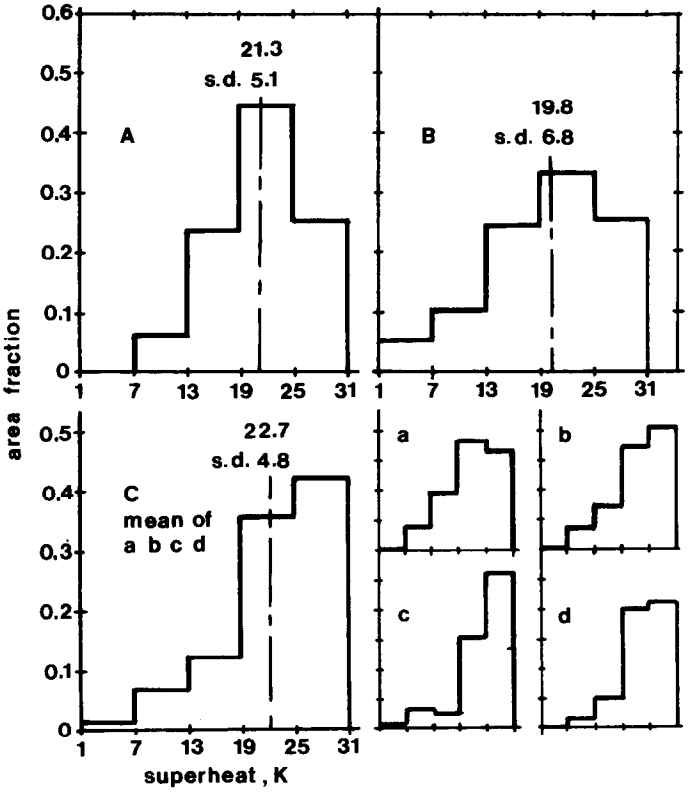

FIG. 4. Superheat–area distributions, Tests A–C.

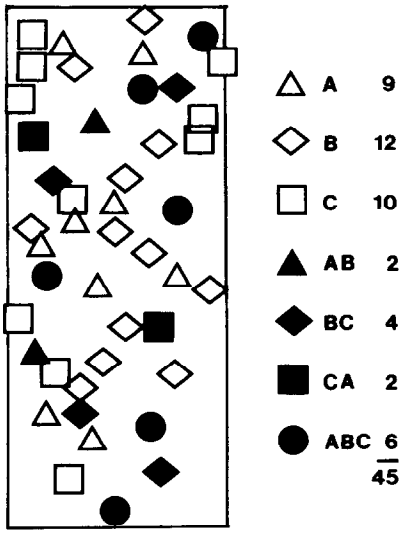

FIG. 5. Nucleation sites, Tests A–C.

suggests that it will be difficult to predict active site densities from surface topography and contact angle only [10]. It may be a consequence of the sensitivity of individual sites to the precise manner in which they are covered with liquid. In experiments on gas bubble nucleation [9, 11, 12], reproducibility depended on stringent precautions (complete initial drying, controlled direction and rate of immersion) which are not normally applied before boiling experiments and cannot be applied during the generation of bubbles. Also in Test C fully-wetted sites may have been activated by trapping vapour [12] from the large bubbles growing at adjacent sites. Alternatively, cleaning with detergent may not have caused the complete displacement of gas and vapour from most of the sites, but may have modified their conditions for activation. In ref. [4] it was suggested that a site is triggered when the local wall temperature exceeds a certain activation superheat. Bubble production then causes gradual local cooling on a timescale long compared to the bubble period: if the local temperature falls below a critical cessation superheat, bubble production stops and is not resumed until the local temperature rises again to the activation superheat. In the boiling experiments with the surface in the poorly-wetted state, sites may have had cessation superheats so low that they were not reached even when sites produced bubbles continuously; when well-wetted, the activation and cessation superheats may have been so close together that the requisite cooling for temporary cessation was achieved in only one or two bubble cycles.

Despite the entirely different boiling processes under different conditions of wetting at the same heat

flux, the mean values of wall superheat are similar, within the accuracy of the crude colour–temperature scaling used in this study. The maximum temperature is higher under the unstable boiling conditions of Test C. Young and Hummel [13] reported an early example of the dependence of wall temperature stability on wettability: low-frequency temperature fluctuations observed during the boiling of water on a well-cleaned, thin stainless steel plate disappeared when the plate was coated with non-wetted spots of PTFE. Extreme forms of instability can occur during the boiling of well-wetting alkali metals on stainless steel [14].

3.2. *Temperature variations in thick plates*

The spacing between active nucleation sites sets the length scale for temperature variations at the boiling surface. The same scale determines the penetration of the time-averaged spatial variations into the solid plate; temporal fluctuations are additionally attenuated on a scale $(\alpha/\omega)^{1/2}$. If the thickness of the plate is much less than these length scales, the variations at the boiling surface are transmitted to its rear surface with little distortion. Thus in Test B the mean spacing between sites is 4.6 mm and the stainless steel plate is 0.13 mm thick so the measurements with liquid crystal should represent the temperature at the boiling surface with a spatial resolution of about 0.2 mm and a flat frequency response over the range 0–20 Hz.

In general the mean spacing between nucleation sites depends on the surface, the fluid and the system pressure. It could lie anywhere between say 0.5 and 10 mm so industrial and experimental boiling systems may have heaters which are 'thin' or 'thick' on this length scale. There is no experimental method of mapping the full range of temperature variations at the boiling surface of a thick plate. Microthermometers (resistance elements or thermocouples) measure local temporal variations but it is impractical to use them in large enough arrays to match the information provided by liquid crystal on thin plates. Instead we estimate the magnitude of the variations on a thick plate by extrapolation from the measurements on a thin plate, assuming the same distribution of surface heat flux. This assumption ignores the distinct possibility of feedback between the temperature variations and the nature of the boiling process.

First an idealized model is fitted to the steady temperature distribution observed in Test B. Following refs. [3, 4], we consider heat flow in a cylinder with cross-sectional area equal to the mean area per nucleation site, that is with radius $S = (\pi N)^{-1/2}$. Lengths are made non-dimensional with respect to S. Heat is generated uniformly internally at a rate equivalent to a mean surface heat flux q and removed by the action of bubbles over the annular region $a \leqslant r \leqslant b$. The fraction of the boiling surface area participating in heat transfer is (b^2-a^2), over which the uniform surface heat flux is $q/(b^2-a^2)$. Heat transfer by enhanced natural convection in the region $b \leqslant r \leqslant 1$ is neglected and the other boundaries of the cylinder are adiabatic. For a thin plate with non-dimensional thickness $d \ll 1$ the axial variations in temperature can be neglected, leading to simple expressions for the time-averaged radial distribution of temperature (see Appendix). In Test B, $S = 2.3$ mm so $d = 0.06$ and the requirement $d \ll 1$ is satisfied. Values of a and b are chosen to match the observed temperature range $\Delta = (130\text{–}104) \pm 1°C$ and spatial mean temperature $T = 120 \pm 1°C$. There is not a unique choice. Making the conventional assumption of uniform heat removal over a circular area of influence (that is with $a = 0$), the required value of $b^2 = 0.66$. The corresponding radius $bS = 1.9$ mm is roughly equal to the estimated bubble departure diameter, again in line with convention. The observations of cool rings (better seen under the large bubbles in Tests A and C than in Test B) suggest that a 'cooled annulus' might be a more realistic model than a 'cooled disc'. The test conditions can be matched by values ranging from $b^2 = 0.4$, $a^2 = 0.25$ to $b^2 = a^2 = 0.35$, still suggesting that the heat transfer occurs mainly in a region outside the periphery of the bubbles. The radial temperature distributions for $b^2 = 0.66$, $a^2 = 0$ and $b^2 = 0.36$, $a^2 = 0.30$ both match the range Δ and mean temperature T in Test B but the corresponding distributions of temperature with respect to area are in poor agreement with the measured distribution, Fig. 6. This may be because the cylindrical-geometry model is a reasonable approximation for sites in a uniform triangular array but is a poor representation of the more distant regions between sites in an irregular array producing bubbles of various sizes.

Whatever its shortcomings, the cylindrical model is at present the only tool available to translate the data for a thin plate to thick plates. Steady conduction in a thick cylinder is solved by standard methods (see Appendix) giving the solutions summarized graphically in refs. [3, 4], with characteristic temperature differences $\Theta = qS/k$. For the heat flux and site density of Test B with $b^2 = 0.66$, $a^2 = 0$ or $b^2 = 0.36$, $a^2 = 0.30$ the amplitude of surface temperature variation Δ on a plate of semi-infinite thickness is 0.48Θ or 0.64Θ, that is 7 or 9 K on a thick stainless steel plate. As amplitude is inversely proportional to thermal conductivity, the corresponding ranges for copper would be only 0.3 or 0.4 K. In circumstances corresponding to small values of b, the temperature variation at the surface of a thick copper plate could be several degrees Kelvin [4].

3.3. *Measurement of mean wall superheat*

The most basic nucleate boiling data define the relationship between heat flux and wall superheat, the boiling curve $q(T)$. The occurrence of temporal variations in wall superheat has long been recognized and, although spatial variations have been disregarded, q and T are implicitly time- and space-averaged values. The demonstration that the spatial variations may, in some circumstances, be large raises

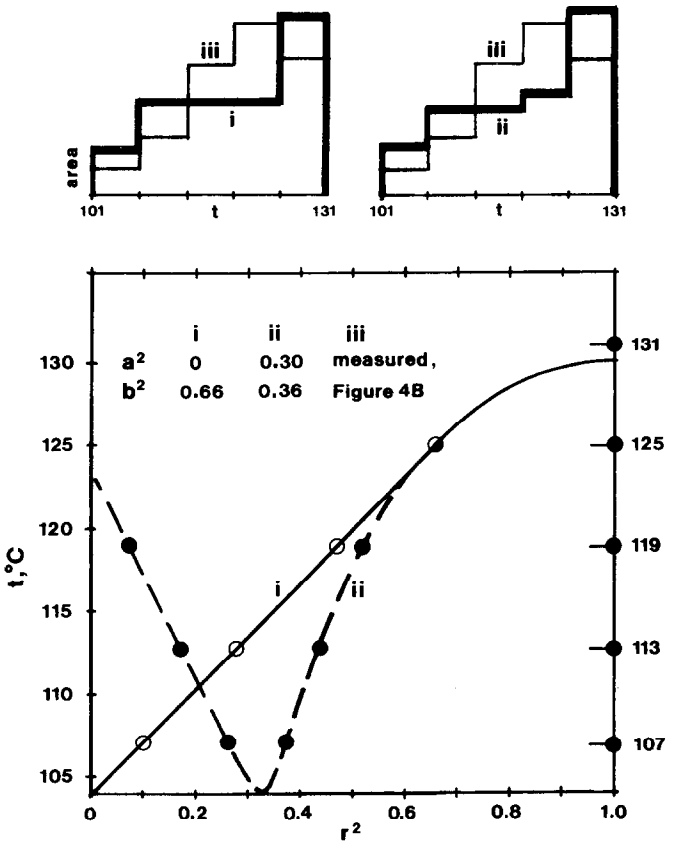

FIG. 6. Temperature distributions, thin-plate model.

two questions: do experiments correctly measure the averaged superheat, and is this quantity sufficient to specify the boiling process?

Many boiling experiments, particularly in flow boiling, use ohmic heating of a thin tube or plate with the wall superheat deduced from temperature measurements by thermocouples attached to the rear, non-boiling surface. Making the plate of thin material of low electrical (and therefore thermal) conductivity reduces the requirement for heavy electrical current. Therefore, the experimental conditions are similar to those used in this paper. Figures 1–3 reveal the difficulty of obtaining a representative value of wall temperature from point-measurements, e.g. from directly-welded thermocouples, even if many are used. Cementing a thermocouple along the surface over an insulating layer provides some averaging by conduction along the thermocouple if the spacing between nucleation sites is small [3]. Better averaging is achieved by attaching a thermocouple to a plate of good conductor large enough to cover several sites; this plate must be electrically insulated from the boiling plate so an outer layer of thermal insulation with well-controlled guard heating is necessary. Alternatively a resistance thermometer grid of fine wire can be cemented to the boiling plate.

The electrical heater itself can be used as a resistance thermometer, e.g. in experiments on boiling on fine wires, which provide little quantitative information applicable to geometries of practical interest. More useful for fundamental studies are experiments in which the electrical heater is a thin (typically 40 nm) semi-transparent conducting film deposited on a glass substrate [15], giving a boiling surface of well-controlled but unusual properties. The relationship between the temperature calculated from the resistance of the heater and the true mean temperature depends on the geometrical disposition of the hot and cold areas. For the simple but extreme case of two equal rectangular areas, one at T_1 and the other at T_2 so $T = (T_1 + T_2)/2$ and $\Delta = T_1 - T_2$, the apparent temperature equals the mean temperature if the current passes through the areas in series but is low by a factor $(1 - \beta\Delta^2/4T)$ if they are in parallel. Taking the thermal coefficient of resistivity $\beta = 4 \times 10^{-3}\ \mathrm{K}^{-1}$ for gold and $\Delta = T = 20$ K, the error is -2% of the mean superheat. In nucleate boiling the error might be smaller, although difficult to quantify. More seriously, the heater is too thin to contribute to lateral conduction which therefore occurs in the electrically-insulating substrate of low thermal conductivity, causing large spatial temperature variations. Although the

conditions of heat input are different, the variations will be the same as those discussed in Section 3.2, of the order of $\Theta/2$. For the distribution of surface heat flux in our representative experiment at 100 kW m^{-2}, the estimated surface temperature variation of 7 K on a thick stainless steel substrate would become 100 K on a glass substrate! This impossibly high estimate indicates that the spatial variations in wall superheat would modify the heat flux distribution towards larger values of b, e.g. by promoting additional nucleation in regions of high superheat. Even organic fluids boiling at low heat fluxes of the order of 10 kW m^{-2} on thin-film heaters with glass substrates are likely to cause substantial variations in surface temperature. Data from this sort of experiment must be interpreted with especial care.

Thick plates with indirect electrical heating on the rear surface are used in pool boiling experiments. The surface temperature and heat flux are calculated from the temperature gradient normal to the boiling surface, measured by embedded thermocouples. If measured correctly, the extrapolation of the gradient gives the mean surface temperature even if the surface heat flux is not uniform (see Appendix) but thermocouples must be placed outside the disturbed region extending a distance of the order of the nucleation site spacing S from the surface. Care is required in experiments designed to study bubble dynamics at very low site densities on polished surfaces, when S may be large.

3.4. *Modelling nucleate boiling*

Mikic and Rohsenow [5] introduced a model for the isolated-bubble regime which has a well-defined physical basis and which has gained wide acceptance. The many variations on their model retain a common structure: the bubble radius R and frequency ω and the density of active nucleation sites N are separately defined by expressions which are then combined in an idealized model for bubble-induced heat transfer. The expressions may be correlations specific to one set of experiments, more general correlations or they may have a theoretical basis. The correlations are recognized to provide averaged values of quantities that vary widely, e.g. bubble size at individual sites and from site to site; the wall superheat, when it appears in a correlation, is given a value which is implicitly a spatial and temporal average, although the existence of large variations is not acknowledged explicitly. Theoretical models, e.g. for bubble frequency [16], may incorporate temporal variations and transient conduction normal to the surface but lateral variations are not considered. The heat-transfer model then uses, in various combinations, quantities which have been averaged separately to calculate the supposed average heat flow into the fluid at every active nucleation site.

The original heat-transfer model, recognized from the outset to be oversimplified [5], assumed spatially uniform transient conduction to cold liquid over an area of influence somewhat larger than the maximum projected area of a bubble. The ratio of these areas K is an empirical 'constant', the value of which actually depends on experimental conditions if it is chosen to optimize the agreement between theory and experiment [17, 18]. The model can be elaborated, e.g. to allow for overlap of areas of influence [19] and additional modes of heat transfer such as microlayer evaporation under bubbles [20]. Transient conduction is usually the major contributor. However, there is an unresolved conflict between the generally satisfactory performance of this model, conventionally calculated with $K = 4$ so that the radius of the area of influence is about twice the maximum bubble radius, and measurements of transient wall temperatures by small arrays of microthermometers [21–23] which have detected little disturbance beyond the radius of the bubble. These experimental observations are supported by one of the few theoretical studies incorporating radial conduction in the wall during bubble growth and detachment [24]. The cold rings in Figs. 1–3 also indicate that heat transfer is more concentrated than the transient-conduction model supposes. It is most important to discover the true pattern of heat removal because it has such a large effect on the calculated magnitude of the spatial variations in wall temperature. In turn, the reduction in wall superheat round a continuously active site means that calculations based on the mean superheat overestimate the heat flow to the fluid.

According to the heat transfer model, the mean heat flux is proportional to the density of active nucleation sites N. In a few experiments this information is obtained by direct observation. More often N must be deduced from a sub-model, such as that proposed by Bergles and Rohsenow [25] and others [26, 27], based on the following physical model.

The boiling surface has a population of potential nucleation sites, each characterized by a single dimension (equivalent radius r') which can be converted to an equilibrium superheat $T_e(r')$. The surface is then specified by the distribution function $N'(r')$, where N' is the cumulative density of sites with radii exceeding r'. A site is activated if the mean wall superheat T (with a correction dependent on the mean heat flux q) exceeds its equilibrium superheat $T_e(r')$.

This model provides the required density of active sites $N(T)$ provided $N'(r')$ is known. On limited evidence [5] it has been assumed that $N'(r')$ can be represented by expressions like

$$N'(r') = C(1/r')^m \tag{1}$$

where m is of the order of 2–6. C and m depend on the microgeometry and wettability of the surface. In the absence of direct measurements of $N'(r')$, their values must be deduced by fitting the complete heat transfer model to experimental measurements of the boiling curve $q(T)$. In effect the model becomes a scheme for correlating boiling curves for a range of conditions by an expression with at least two adjustable coefficients.

The model can sometimes do this very successfully [28]. However, there is some very limited evidence from the direct measurement of $N'(r')$ by gas bubble diffusion on the inner surface of a drawn tube [29] that the density of small sites does not increase without limit as $r' \to 0$, as implied by equation (1). Many more determinations of $N'(r')$ should be performed on a wide variety of surfaces to establish a suitable general form for the distribution function.

Despite the successes of the heat transfer model, there is much evidence that the physical assumptions behind the sub-model for active nucleation site density are grossly oversimplified.

(i) *Boiling curve hysteresis.* Hysteresis is generally associated with well-wetting fluids, e.g. ref. [30]. The site density model, with its simple criterion for activation, cannot distinguish between states reached by increasing or decreasing the mean wall superheat and heat flux. It might be argued that the model only applies under the conditions of decreasing heat flux often employed in laboratory experiments. This would imply that the condition for site activity is actually the condition for maintaining activity, and that some different model is required to describe the problems of initiating boiling, which can have important consequences in industrial applications ranging from cryogenic heat exchangers to cooling of electronic components.

(ii) *Interaction between sites.* The model requires sites to be so far apart that they do not interact and the wall superheat at each site to be equal to the mean superheat, requirements which may conflict. If sites are randomly distributed, some should be close together even when the average spacing is large. Eddington and Kenning [12] showed that in subcooled flow boiling the random distribution was distorted by an inhibiting process within about two bubble radii of an active site. Judd and co-workers [17, 31, 32] observed inhibition and promotion near active sites in pool boiling. This is indirect evidence for variations in wall superheat large enough to influence nucleation, although disturbances could be propagated through the fluid rather than the wall.

(iii) *Irregular behaviour of sites.* In boiling at constant heat flux the model supposes that all activated sites remain active, producing bubbles continuously at a steady frequency. Myers and co-workers [2, 8, 33] described the intermittent behaviour of nucleation sites in pool boiling, also seen in Test A of this paper and in an extreme form in Test C. Intermittency reduces the number of sites contributing to heat transfer at any instant under nominally steady conditions. Following increases in heat flux and mean wall superheat the sites previously active should, according to the model, all remain active and be reinforced by additional sites in a regular and progressive manner. The behaviour observed by del Valle and Kenning [18] during successive increases in heat flux in subcooled flow boiling was much more complex. Although there was a net increase in the number of active sites, some sites active at low heat flux were inactive at higher flux. (In the light of current work, it should be noted that the method of observation in those experiments would not have detected a possible influence of intermittency over long periods: sites were detected by high-speed photography over a sampling period of less than 0.5 s.)

This paper has provided experimental evidence and theoretical arguments that spatial variations in wall superheat occur in many boiling systems. These variations provide qualitative explanations for the phenomena listed above. They also invalidate the physical modelling underpinning the model for active site density $N(T)$.

Consider the consequences of a small increase in heat flux accompanied by a small increase in mean wall superheat from T to $T+\mathrm{d}T$. According to the model, the density of active sites increases by an amount $\mathrm{d}N$ proportional to $\mathrm{d}N/\mathrm{d}T$ at the mean value T, Fig. 7(a). The slope of the boiling curve $\mathrm{d}q/\mathrm{d}T$ at T is also closely linked to $\mathrm{d}N/\mathrm{d}T$ at T through the heat transfer model. Actually the wall superheat ranges about the mean value T by a relatively large amount Δ. Supposing for the moment that $N(T)$ applies if the local superheat is used instead of the mean value, $\mathrm{d}N$ might be expected to depend on $\mathrm{d}N/\mathrm{d}T$ at the maximum superheat, Fig. 7(b). This is an over-simplification since the higher probability of activating new sites in the regions of higher than average superheat must be weighted with the probability of there being potential sites in those regions. In order to calculate $\mathrm{d}N$ it is necessary to know the distribution of superheat with respect to area, which depends on N, q and the properties of the wall.

Next consider the difficulties that arise even when the model is applied on a local basis. Suppose that a small increase in heat supply is just sufficient to activate a new nucleation site at a local superheat T_a. If the site produces bubbles at a finite rate the step increase in cooling in the immediate vicinity of the site causes a reduction in the local superheat, unless the boiling plate has infinite thermal conductivity. The new site must be able to survive this reduction if it is to remain active. The specification of the site must be expanded to include the superheat T_c at which it ceases to produce bubbles. If the local superheat stabilizes above T_c the site remains continuously active. If the superheat falls to T_c, the site switches off: with its cooling effect removed, the local superheat rises again to T_a, reactivating the site so that it becomes intermittently active. The disturbances in the wall superheat pattern round the new site may also affect adjacent sites, causing inhibition, intermittency or even promoting activity by the elimination of another site.

The simple model with uniform superheat presents a picture of a population of active nucleation sites which is static under steady-state conditions and which changes in an orderly and regular manner as

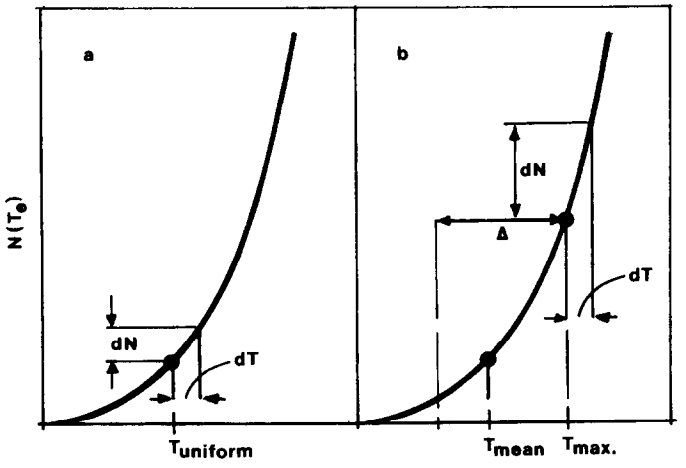

FIG. 7. Site density model (a) without and (b) with spatial variations in superheat.

the heat flux changes. This may approximate to the behaviour of real systems with thick walls of high conductivity, such as copper. Sultan and Judd [34] reported regular increases in site density with increasing heat flux for water boiling on copper, although it should be noted that their method of detecting sites by traversing a probe through the fluid would not have detected long-period intermittency. The conditions for near-uniform superheat (wall thickness large compared to the site separation S and mean superheat $T \gg qS/k$) are not satisfied in many experimental and industrial boiling systems. Then a model which is to represent the essential physics of nucleate boiling with a mixture of steady and intermittent sites must have the following features:

(a) consideration of local superheats to determine the activity of sites and their contribution to heat transfer;

(b) specification of sites by their conditions for activation and cessation;

(c) allowance for the effect of intermittency on the overall (space- and time-averaged) heat flux.

Intermittency disrupts the simple proportionality between mean heat flux q and the total population of active sites N. A simple extended model (sites specified by activation superheat T_a, cessation superheat T_c and constant heat flow whilst active ϕ) was used in ref. [4] to demonstrate that even idealized systems with only two types of site can generate quite complex boiling curves.

3.5. *Do we need a better model?*

If the simple (uniform superheat) model does not have a sound mechanistic basis, its status is downgraded to just another correlation scheme. As noted in Section 3.4, it may be quite successful in that role but it faces competition from other schemes, e.g. using reduced properties [35]. All correlations face difficulties in representing the influence of the condition of the boiling surface. We may suspect, from the discussion in this paper, that the difficulties also hide some influence of the bulk properties of the wall.

The price of realism is complexity: much more input data are required, such as the size distributions of sites with different ratios T_a/T_c. A criticism of the existing model can be based, as here, on very limited observations. Assembling sufficient data to construct a better mechanistic model is a much bigger enterprise. It may be difficult to fund in the present financial climate if the final result is a prediction of the boiling curve which is only marginally better than empirical correlations. The payoff from better models may come in systems where the variations in wall superheat have important direct consequences: hysteresis which limits the operability of fluid–fluid heat exchangers designed to run at low temperature differences, effects on corrosion and fouling, thermal stresses and the reliability of devices cooled by nucleate boiling.

4. CONCLUSIONS

(i) Experimental and theoretical evidence has been presented that large spatial variations in wall superheat are to be expected in nucleate boiling on thin-walled tubes and plates and on thick plates made of materials of moderate thermal conductivity, like stainless steel.

(ii) The variations can cause errors in the measurement of mean wall superheat by some conventional techniques.

(iii) Existing mechanistic models which assume uniformity of wall superheat are only valid in the limit of boiling on thick plates of high conductivity, like copper. They do not represent correctly the mechanisms controlling the density of active nucleation sites in many experimental and industrial systems.

(iv) A realistic model must incorporate the effects of local wall superheat on bubble site activity, allowing for the possibility of intermittency. Sites must be described by two characteristic superheats, one for activation and one for cessation.

Acknowledgement—This work was performed without funding. Dr H. J. Coles of Manchester University generously provided a sample of thermochromic liquid crystal of the required specification.

REFERENCES

1. V. K. Dhir, Nucleate and transition boiling heat transfer under pool and external flow conditions, *Proc. 9th Int. Heat Transfer Conf.*, Jerusalem, Vol. 1, pp. 129–156 (1990).
2. T. Raad and J. E. Myers, Nucleation studies in pool boiling on thin plates using liquid crystals, *A.I.Ch.E. Jl* **17,** 1260–1261 (1971).
3. D. B. R. Kenning, Wall temperatures in nucleate boiling, Oxford University Engineering Laboratory Report No. 1530/84 (1984).
4. D. B. R. Kenning, Wall temperatures in nucleate boiling: spatial and temporal variations, *Proc. 9th Int. Heat Transfer Conf.*, Jerusalem, Vol. 3, pp. 33–38 (1990).
5. B. B. Mikic and W. M. Rohsenow, A new correlation of pool boiling data including the effect of heating surface characteristics, *ASME J. Heat Transfer* **91,** 245–250 (1969).
6. P. T. Ireland and T. V. Jones, The response time of a surface thermometer employing encapsulated thermochromic liquid crystals, *J. Phys. E. Sci. Instrum.* **20,** 1195–1199 (1987).
7. P. Bonnett, Applications of liquid crystals in aerodynamic testing, Ph.D. Thesis, Department of Engineering Science, Oxford University (1989).
8. J. E. Myers, Short-lived sites in nucleate boiling, *A.I.Ch.E. Jl* **31,** 1441–1445 (1985).
9. R. I. Eddington and D. B. R. Kenning, The effect of contact angle on bubble nucleation, *Int. J. Heat Mass Transfer* **22,** 1231–1236 (1979).
10. S. R. Yang and R. H. Kim, A mathematical model of the pool boiling nucleating site density in terms of the surface characteristics, *Int. J. Heat Mass Transfer* **31,** 1127–1135 (1988).
11. R. I. Eddington, D. B. R. Kenning and A. Korneichev, Comparison of gas and vapour bubble nucleation on a brass surface in water, *Int. J. Heat Mass Transfer* **21,** 855–862 (1978).
12. R. I. Eddington and D. B. R. Kenning, The prediction of flow boiling populations from gas bubble nucleation experiments, *Proc. 6th Int. Heat Transfer Conf.*, Toronto, Vol. 1, pp. 275–280 (1978).
13. R. K. Young and R. L. Hummel, Improved nucleate boiling heat transfer, *Chem. Engng Prog.* **60,** 53–58 (1964).
14. P. J. Marto and W. M. Rohsenow, Nucleate boiling instability of alkali metals, *ASME J. Heat Transfer* **88,** 183–195 (1966).
15. E. Oker and H. Merte, Semi-transparent gold film as simultaneous surface heater and resistance thermometer for nucleate boiling studies, *ASME J. Heat Transfer* **103,** 65–68 (1981).
16. M. S. M. Shoukri and R. L. Judd, A theoretical model for bubble frequency in nucleate boiling including surface effects, *Proc. 6th Int. Heat Transfer Conf.*, Toronto, Vol. 1, pp. 145–150 (1978).
17. R. L. Judd and C. H. Lavdas, The nature of nucleation site interaction, *ASME J. Heat Transfer* **102,** 461–464 (1980).
18. V. H. del Valle M. and D. B. R. Kenning, Subcooled flow boiling at high heat flux, *Int. J. Heat Mass Transfer* **28,** 1907–1920 (1985).
19. D. B. R. Kenning and V. H. del Valle M., Fully developed nucleate boiling: overlap of areas of influence and interference between bubble sites, *Int. J. Heat Mass Transfer* **24,** 1025–1032 (1981).
20. R. L. Judd and K. S. Hwang, A comprehensive model for nucleate pool boiling heat transfer including microlayer evaporation, *ASME J. Heat Transfer* **98,** 623–629 (1976).
21. M. G. Cooper and A. J. P. Lloyd, Transient local heat flux in nucleate boiling, *Proc. 3rd Int. Heat Transfer Conf.*, Chicago, Vol. 1, p. 193 (1966).
22. V. I. Subbotin, D. N. Sorokin, A. A. Tzyganok and A. A. Gribov, Investigation of vapour bubbles effect on temperature of heat transferring surface at nucleate boiling, *Proc. 5th Int. Heat Transfer Conf.*, Tokyo, Vol. 4, pp. 55–59 (1974).
23. S. A. Barakat and G. E. Sims, Heat transfer in pool barbotage, *Proc. 6th Int. Heat Transfer Conf.*, Toronto, Vol. 1, pp. 127–132 (1978).
24. H. Beer, P. Burow and R. Best, Bubble growth, bubble dynamics and heat transfer in nucleate boiling. In *Heat Transfer in Boiling* (Edited by E. Hahne and U. Grigull), Chap. 2. Hemisphere, Washington, DC (1977).
25. A. E. Bergles and W. M. Rohsenow, The determination of forced-convection surface-boiling heat transfer, *ASME J. Heat Transfer* **86,** 365–372 (1964).
26. Y. Y. Hsu, On the size range of active nucleation cavities on a heating surface, *ASME J. Heat Transfer* **84,** 207–216 (1962).
27. D. B. R. Kenning and M. G. Cooper, Flow patterns near nuclei and the initiation of boiling during forced convection heat transfer, *Proc. I MechE* **180**(3C), 112–123 (1965–66).
28. K. Bier, D. Gornenflo, M. Salem and Y. Tanes, Pool boiling heat transfer and size of active nucleation centres for horizontal plates with different surface roughness, *Proc. 6th Int. Heat Transfer Conf.*, Toronto, Vol. 1, pp. 151–156 (1978).
29. Y. Aounallah, Heat transfer in annular two-phase flow, Ph.D. Thesis, Oxford University (1982).
30. H. Toral, D. B. R. Kenning and R. A. W. Shock, Flow boiling of ethanol/cyclohexane mixtures, *Proc. 7th Int. Heat Transfer Conf.*, Munchen, Vol. 4, pp. 225–260 (1982).
31. M. Sultan and R. L. Judd, Interaction of the nucleation phenomena at adjacent sites in nucleate boiling, *ASME J. Heat Transfer* **105,** 3–9 (1983).
32. R. L. Judd, On nucleation site interaction, *ASME J. Heat Transfer* **110,** 475–478 (1988).
33. J. E. Sgheiza and J. E. Myers, Behaviour of nucleation sites in pool boiling, *A.I.Ch.E. Jl* **31,** 1605–1613 (1985).
34. M. Sultan and R. L. Judd, Spatial distribution of active sites and bubble flux density, *ASME J. Heat Transfer* **100,** 56–62 (1978).
35. M. G. Cooper, Heat flow rates in saturated nucleate pool boiling—a wide-ranging examination using reduced properties. In *Advances in Heat Transfer*, Vol. 16, pp. 157–239. Academic Press, New York (1984).
36. H. S. Carslaw and J. C. Jaeger, *Conduction of Heat in Solids*. Clarendon Press, Oxford (1959).

APPENDIX

Consider the temperature field in a cylindrical region of radius S round a nucleation site, Fig. A1. Lengths are made nondimensional with respect to S, temperatures with respect to $\Theta = qS/k$. Time-dependent variations are assumed steady-periodic so that the time-averaged temperature field is described by the steady conduction equation. Heat is supplied at a rate equivalent to a mean surface heat flux q by one of the following methods: uniform internal generation,

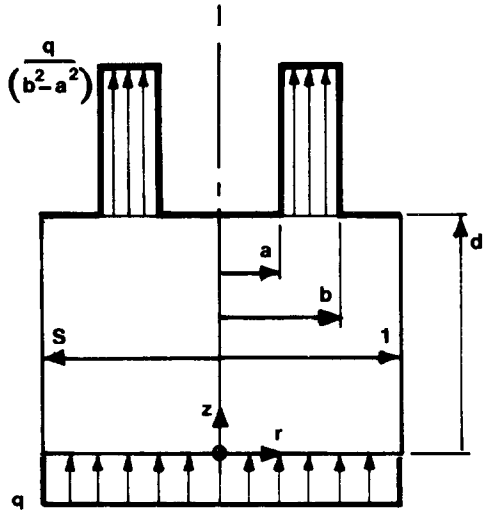

FIG. A1. Domain for steady-conduction model.

uniform supply over the rear face of the cylinder, uniform supply over the front face of the cylinder (e.g. by an electrical resistance heater of microscopic thickness). The heat flux from the front face to the boiling fluid is the sum of the mean flux q and a perturbation $f(r)$ which makes no net contribution to the heat flow

$$\int_0^1 2\pi r f(r)\,\mathrm{d}r = 0. \tag{A1}$$

The temperature field is the sum of the one-dimensional field $t_1(z)$, which depends on q and the method of heating and the perturbation $t(r, z)$ due to $f(r)$ with adiabatic conditions on the other boundaries of the cylinder and no internal heat generation. We note that the variations in surface temperature do not depend on the method of supplying heat, provided the supply is uniform.

We have chosen a model in which heat flow to the boiling fluid is confined to the annular surface region $a \leqslant r \leqslant b$, so

$$f(r) = -q, \quad 0 \leqslant r \leqslant a \quad \text{and} \quad b \leqslant r \leqslant 1$$
$$= q\left[\frac{1}{(b^2-a^2)} - 1\right], \quad a \leqslant r \leqslant 1. \tag{A2}$$

The perturbation temperature field must satisfy

$$\frac{\partial^2 t}{\partial r^2} + \frac{1}{r}\frac{\partial t}{\partial r} + \frac{\partial^2 t}{\partial z^2} = 0 \tag{A3}$$

$$r = 1, \quad \frac{\partial t}{\partial r} = 0; \quad z = 0, \quad \frac{\partial t}{\partial z} = 0 \tag{A4}$$

$$z = d, \quad \frac{\partial t}{\partial z} = -1, \quad 0 \leqslant r \leqslant a, \quad b \leqslant r \leqslant 1$$
$$= \frac{1}{(b^2-a^2)} - 1, \quad a \leqslant r \leqslant b. \tag{A5}$$

Solving by standard methods, e.g. Chaps. 7 and 8 of ref. [36]

$$t = -\frac{2}{(b^2-a^2)}\sum_{n=1}^{\infty} \frac{\cosh(\alpha_n d)[bJ_1(\alpha_n b) - aJ_1(\alpha_n a)]J_0(\alpha_n r)}{\alpha_n^2 \sinh(\alpha_n d)[J_0(\alpha_n 0)]^2} \tag{A6}$$

where α_n are the positive roots of $J_1(\alpha_n) = 0$. Since

$$\int_0^1 r J_0(\alpha_n r)\,\mathrm{d}r = J_1(\alpha_n) = 0 \tag{A7}$$

the perturbation field makes no contribution to the mean temperature on the heat transfer surface $z = d$. Consequently the one-dimensional corrections conventionally made in boiling experiments to deduce the surface temperature from remote measurements do give the mean value correctly.

When $d \ll 1$ temperature variations in the direction normal to the surface can be neglected and the surface temperature relative to its mean value is given by

$$0 \leqslant r \leqslant a: \quad 4(t+T_0)d = -r^2 \tag{A8}$$

$$a \leqslant r \leqslant b: \quad 4(t+T_0)d = \frac{a^2}{(b^2-a^2)}\left[\frac{r^2}{a^2}(1+a^2-b^2) - \ln\left(\frac{r^2}{a^2}\right) - 1\right] \tag{A9}$$

$$b \leqslant r \leqslant 1: \quad 4(t+T_0)d = 1 - r^2 + \ln r^2 + \left[\frac{a^2 \ln a^2 - b^2 \ln b^2}{(b^2-a^2)}\right] \tag{A10}$$

where

$$4T_0 d = \left[\frac{a^2 \ln a^2 - b^2 \ln b^2}{(b^2-a^2)}\right] - \frac{(1-a^2-b^2)}{2}. \tag{A11}$$

CONFIGURATION DE TEMPERATURE PARIETALE DANS L'EBULLITION NUCLEE

Résumé—Les configurations de température à l'arrière d'une mince plaque chauffée en acier inoxydable pendant l'ébullition nuclée d'eau en réservoir sont mesurées avec un cristal liquide thermochrome. Il est montré que les variations spatiales qui sont de larges fractions de la surchauffe moyenne de la paroi sont rencontrées dans de nombreuses applications expérimentales et industrielles de l'ébullition. Elles causent des erreurs dans la mesure de la surchauffe moyenne de la paroi par quelques méthodes conventionnelles. Les modèles mécanistes établis qui supposent l'uniformité de la surchauffe de la paroi ne peuvent représenter correctement les mécanismes contrôlant la densité et l'activité intermittente des sites de nucléation des bulles sur la paroi ayant une conductivité thermique finie. Les caractères essentieles d'un modèle réaliste sont décrits.

VERTEILUNG DER WANDTEMPERATUR BEIM BLASENSIEDEN

Zusammenfassung—Mit Hilfe thermochromer Flüssigkristalle wird die Temperaturverteilung an der Rückseite einer dünnen, beheizten Platte aus rostfreiem Stahl gemessen, wenn an der Vorderseite Blasensieden von Wasser stattfindet. Es wird gezeigt, daß bei vielen Versuchsanordnungen und industriellen Anwendungen des Siedens starke räumliche Temperaturunterschiede zu erwarten sind. Deren Größenordnung entspricht einem größen Bruchteil der mittleren Wandüberhitzung. Diese Temperaturunterschiede können bei einigen herkömmlichen Meßverfahren zu Fehlern bei der Bestimmung der mittleren Wandüberhitzung führen. In herkömmlichen mechanistischen Modellen wird von einer gleichförmigen Wandüberhitzung ausgegangen. Derartige Modelle sind außerstande, die Vorgänge richtig zu beschreiben, welche die Dichte und die intermittierende Aktivität von Blasenkeimstellen an einer Wand endlicher Wärmeleitfähigkeit bestimmen. Die grundlegenden Charakteristika eines realistischen Modells werden beschrieben.

ПРОФИЛИ ТЕМПЕРАТУР СТЕНКИ ПРИ ПУЗЫРЬКОВОМ КИПЕНИИ

Аннотация—С использованием термохромного жидкого кристалла определяются профили температур на задней стенке тонкой нагретой пластины из нержавеющей стали при пузырьковом кипении воды в большом объеме. Показано, что во многих случаях экспериментального и промышленного применения кипения ожидается возникновение пространственных изменений в определении средней величины перегрева стенки, что может привести к погрешностям его измерений общепринятыми методами. Модели, разработанные в предположении однородности перегрева стенки, не могут адекватно описывать процессы, которые регулируют плотность и интенсивность образования пузырьков на стенках с конечной теплопроводностью. Описываются основные особенности предлагаемой модели.